

Modulating the Physical Properties of Sunflower Oil and Sorbitan Monopalmitate-Based Organogels

Beauty Behera,¹ Sai S. Sagiri,¹ Kunal Pal,¹ Anand Srivastava²

¹Department of Biotechnology & Medical Engineering, National Institute of Technology, Rourkela-769008, Odisha, India

²Department of Pharmaceutical Engineering, Institute of Technology, Banaras Hindu University, Varanasi -221005, Uttar Pradesh, India

Correspondence to: K. Pal (E-mail: pal.kunal@yahoo.com)

ABSTRACT: The present study deals with the modulation of the sunflower oil (SO) and sorbitan monopalmitate (SM) organogels using water. The gels were prepared by heating either SO–SM mixture or SO–SM–water mixture at 60°C and subsequently cooling the mixture to room temperature. The gels were characterized by microscopy (light and electron), Fourier transform infrared (FTIR) spectroscopy, X-ray diffraction (XRD), differential thermal analysis, rheometry, pH, dc impedance, hemocompatibility, and antimicrobial studies. The gels without water (G) were found to be pale yellow in color while gels containing water (GW) were white in color. Both types of gels were thermoreversible in nature. The microscopic analysis revealed that clusters of rod-shaped tubules were responsible in the formation of network. GW also showed the presence of water droplets encapsulated within the networked structure. FTIR studies indicated the presence of intermolecular hydrogen bonding, responsible for gel formation. Gel-to-sol transition temperatures (T_{gs}) of the GW gels were higher than G gels, which might be accounted to the higher crystallinity of the GW gels. XRD studies confirmed the higher crystallinity of the GW gels. The gels showed pseudoplastic flow behavior and were hemocompatible in nature. Ciprofloxacin-loaded gels showed good anti-microbial properties against *Bacillus subtilis*. Based on the preliminary results, the developed gels may be used as delivery vehicles for various bioactive agents. © 2012 Wiley Periodicals, Inc. *J. Appl. Polym. Sci.* 000: 000–000, 2012

KEYWORDS: organogel; sorbitan monopalmitate; conformation; pseudoplastic; hemocompatibility

Received 17 December 2011; accepted 11 February 2012; published online 00 Month 2012

DOI: 10.1002/app.37506

INTRODUCTION

Of late, there has been an increased use of vegetable oils for the production of various food, cosmetic, and pharmaceutical products. This is mainly due to the functional and beneficial properties of vegetable oils apart from their inherent physical stability.¹ One such product is thermo-reversible organogels, semi-solid product having apolar phase as the continuous phase.² They are often also known as lipogels or oleogels.³ They are usually prepared by dissolving low-molecular weight gelators (MW < 3000), in concentration above critical gelation concentration (CGC), in hot apolar liquids followed by lowering the temperature of the hot gelator solution below the sol-to-gel transition temperature ($T_{sol-to-gel}$).⁴ These gels are generally viscoelastic in nature. The properties of these gels have been found to be dependent on the composition of the oils and fats used.⁵ Though various studies on the use of

fatty acid esters as organogelators have been reported, unfortunately not much emphasis has been paid on the use of sorbitan monopalmitate (SM) as an organogelator. SM, a fatty acid derived ester (Figure 1), is basically a non-ionic emulsifier having a hydrophilic lipophilic balance (HLB) of 6.7, which makes it a good candidate to promote water-in-oil emulsion.⁷ It has been reported that SM can help developing semi-solid formulations by immobilizing apolar liquid.⁸

Sunflower oil (SO) is highly rich in vitamin E and omega-6 polyunsaturated fatty acids (prone to oxidative degradation). The degradation may be reduced by converting them into highly cohesive gel matrix.⁹ Due to this property, SO has been often used in devising matrices for controlled delivery of bioactive agents.⁶

Taking inspiration from the above, attempts have been made to develop organogels using SM as the organogelator and SO as the apolar liquid. Further attempts were also made to improve

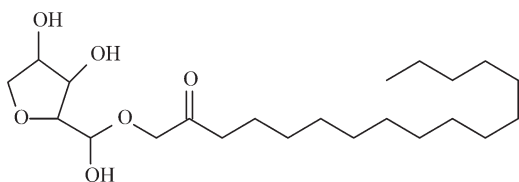


Figure 1. Structure of span 40. Redrawn from Ref. 6.

the stability of the SM-SO organogels by incorporating water into the gelled structure.

MATERIALS AND METHODS

Materials

SM (Span 40) and ciprofloxacin were purchased from Loba chemi, Mumbai, India and Fluka, China, respectively. SO (edible grade) was procured from the local market, India. Microbial culture of *Bacillus subtilis* (NCIM 2699) was obtained from NCIM, Pune, India. Double distilled water was used throughout the study.

Sample Preparation

A homogenous solution of SM in SO was prepared by stirring the mixture at 60°C. The transparent solution was subsequently cooled to room temperature for 2 h. The concentration of SM was varied from 1% (w/w) to 25% (w/w) to find out the CGC. CGC is the minimum concentration of SM required to gel SO.¹⁰ The CGC was found to be 18% (w/w) and the sample was regarded as gels without water (G). The phenomena of gelation was confirmed by inverted tube method (Figure 2).¹¹ To study the effect of water on the properties of water, 5 g water was added to 5 g G, kept on stirring at 60°C. The samples were cooled to room temperature for 2 h and were regarded as gels containing water (GW).

Optical Microscopy

The gels, both G and GW, were observed under a light microscope (Model CX21FS1, Olympus, India) to understand the microstructure of the gels.

Scanning Electron Microscopy

The gels were analyzed under scanning electron microscope (JEOL, JSM-6390, Japan). The gels were converted into xerogels by drying for 6 h under high vacuum. The xerogels were then sputter-coated with platinum before subjecting the samples for analysis.

FTIR Spectroscopy

SM, SO, and both the gels were analyzed by attenuated total reflection infrared (ATR-IR) spectrometer (AlphaE ATR-FTIR, Bruker, USA) in the range of 450–4000 cm⁻¹.

Gel-Sol Transition Temperature

Gel-sol transition temperature (T_{gs}) was determined using the tube inversion method. The samples were placed in a water bath and heated slowly from 35°C to 80°C. Each of the samples was equilibrated for 5 min at temperature intervals of 5°C. The T_{gs} was analyzed by inverting the vial after each incubation period.^{11,12} The T_{gs} was characterized as the temperature where the gels started to flow under gravity when the tubes were inverted. All the experiments were carried out in duplicate.

XRD Analysis

SM, SO, and both the gels were subjected to X-ray diffraction (PW3040, Philips, Holland) using a monochromatized Cu K α

radiation ($\lambda = 0.154$ nm) in the range of 5°–50° 2 θ . The scan-rate for the analysis was 2° 2 θ /min.

Thermal Behavior of Gels

The gels were subjected to differential thermal analysis (DTA) using H-Res/modulated DTA 2950 (TA instruments, USA) over a temperature range of 25–300°C at a heating rate of 6 °C/min.

Rheological Measurement

The rheological properties of the gels were studied using controlled stress cone-plate viscometer (Bohlin visco 88, Malvern, UK). All measurements were made on freshly prepared samples. Cone and plate geometry was used. The cone had dimension of cone angle of 5.4° and diameter of 30 mm. The gap between the cone and the plate was set at 0.15 mm. Solvent trap was used to prevent the moisture loss. All the measurements were carried out at room temperature.

pH

The pH of the samples was determined by pH meter (Model 132E, EI products, India). For determination of pH the probe was simply dipped into freshly prepared gels.¹³

DC Impedance Measurement

The dc impedance of the gels were measured using an in-house made dc impedance meter. The impedances of the gels were calculated by using eq. (1):

$$Z = \frac{V}{I} \quad (1)$$

where, Z = impedance, V = voltage drop across the sample, and I = current passing through the sample.

Hemolysis Study

The gels, placed in a dialysis tubing (MW cut-off = 12kda), were equilibrated in 50 mL of saline at 37°C for 30 min. 0.5 mL aliquots of this solution was mixed with 0.5 mL of citrated goat blood diluted with normal saline (prepared in 4 : 5 ratio), followed by the addition of normal saline (9 mL). The positive control (+ve) was prepared by adding 0.5 mL of 0.1N hydrochloric acid to 0.5 mL of diluted blood whereas the negative control (–ve) was prepared by adding 0.5 mL of saline to 0.5 mL of diluted blood. The final volume was made up to 10 mL using saline. Thereafter, the test, the +ve control, and the –ve control were incubated at 37°C for 1 h. After incubation, the samples were subsequently centrifuged at 3000 rpm for 10 min. The supernatant was siphoned off and analyzed at 545 nm using a UV-visible spectrophotometer (UV 3200 double beam, Labindia). % haemolysis was calculated from the following equation:

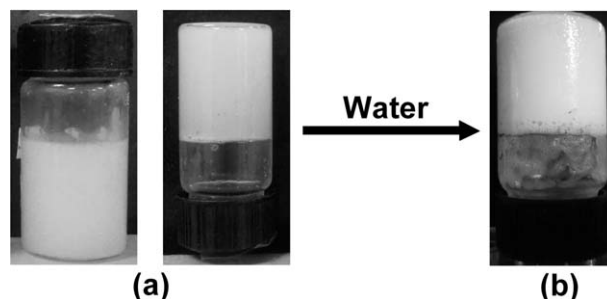


Figure 2. Inverted tube method showing the gel formation (a) G, (b) GW.

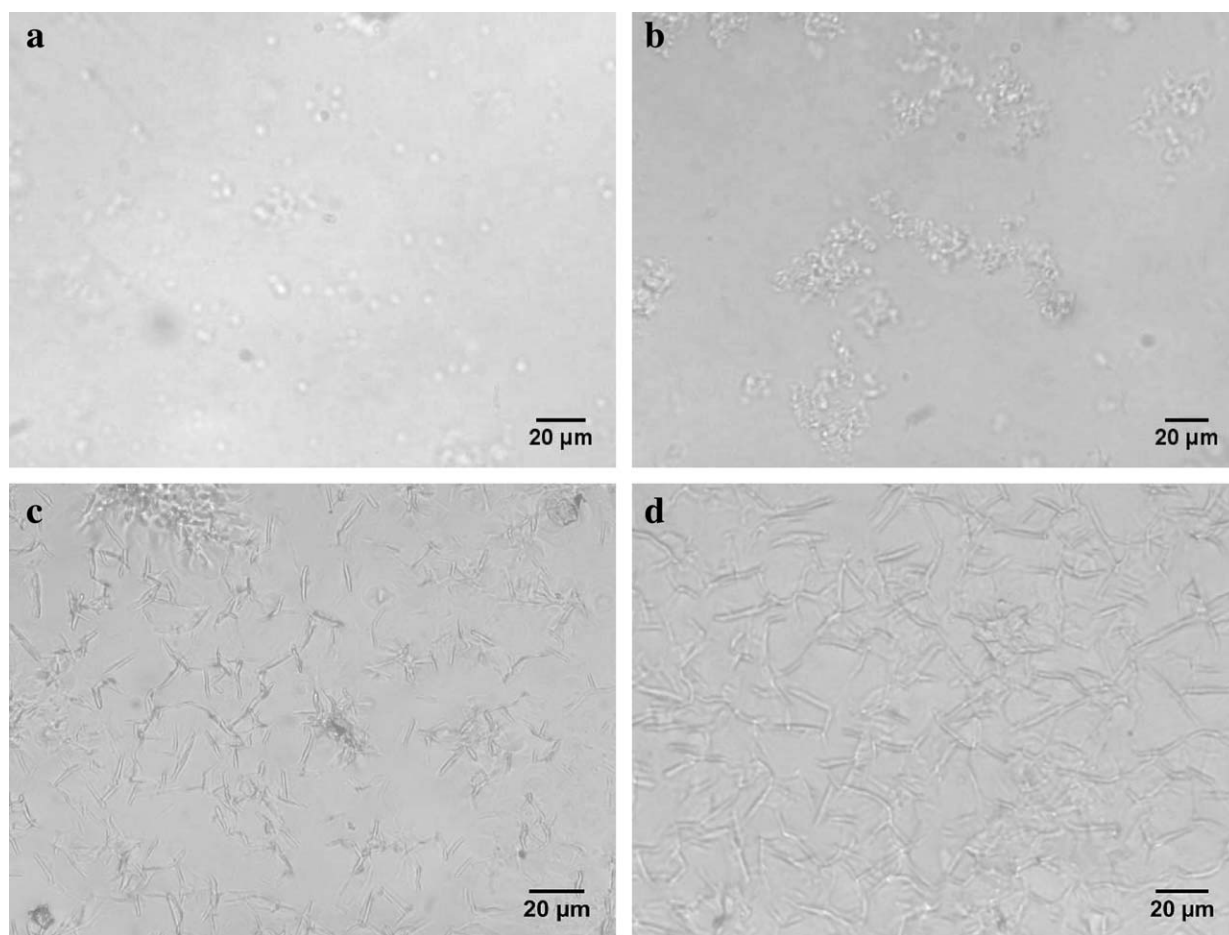


Figure 3. Light microscopy of organogels under high magnification showing the mechanism of gel formation with increase in concentration of gelators (a) 2%, (b) 5%, (c) 10%, and (d) 18% of gelator.

$$\% \text{ Hemolysis} = \frac{\text{OD}_{\text{Test}} - \text{OD}_{\text{Negative}}}{\text{OD}_{\text{Positive}} - \text{OD}_{\text{Negative}}} \times 100 \quad (2)$$

where, OD_{Test} = optical density of test sample, $\text{OD}_{\text{Positive}}$ = optical density of +ve control, and $\text{OD}_{\text{Negative}}$ = optical density of –ve control.

Antimicrobial Studies

The efficacy of the gels as a carrier for antimicrobial agents was studied against *B. subtilis*, gram positive bacteria. The samples for this study were prepared by incorporating 1% (w/w) ciprofloxacin to G and GW gels and the samples were regarded as GD and GWD, respectively. The antimicrobial activity was determined by agar diffusion assay. Fresh colonies of bacterial strains were inoculated in 100 mL of nutrient broth and incubated in a shaker incubator for overnight at 37°C. The final volume was adjusted to 5×10^5 cfu/mL. The inoculum was applied to agar plates with a sterilized spreader.¹⁴ Wells of diameter 5 mm were bored with a borer and then filled with predetermined amount of gels. Wells containing drug was used as positive control. The culture plates were incubated at 37°C \pm 1°C for 24 h.

Stability Studies

The G and GW gels were subjected to 25°C/60% relative humidity (RH) and were observed visually for syneresis associated with phase separation.¹⁵

RESULTS AND DISCUSSION

Light Microscopy

The microscopic structures revealed that individual tubules of SM joined together to form a networked structure. Similar mechanism of self-assembly of tubules of the organogelators has also been reported by Li et al. (2007).¹⁶ Figure 3 shows the micrographs as the concentration of gelator was increased. The micrographs showed the presence of circular structures at 2% (w/w), which may be accounted to the formation of reverse micelles by the SM molecules at lower concentration. The sample containing 5% (w/w) showed clusters of particles of SM having irregular size and shape. As the concentration of the gelator was increased to 10% (w/w), needle-shaped crystals were observed. With the further increase in the gelator concentration to CGC, these needle-shaped crystals grew in size and formed interconnecting networked structures. These interconnected networked structures were responsible for the immobilization of the apolar phase which may be attributed to the surface active interactions amongst the gelator and apolar phase.¹⁷ The gelator molecules formed fiber-like structures which entangled with each other to form a 3D networked structure (Figure 4). GW gel showed uniform distribution of the water droplets throughout the gelled structure (Figure 5).

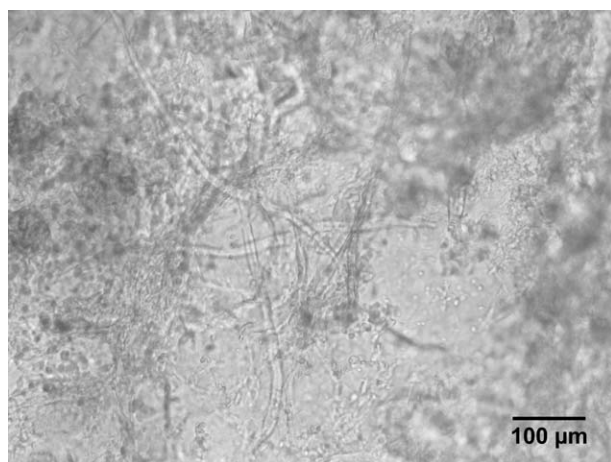


Figure 4. Light microscopy of G at low magnification showing the fibrillar arrangement of the gelator responsible for gel formation.

Scanning Electron Microscopy

The xerogels of G and GW gels were studied using scanning electron microscope to confirm the structure of the gels as visualized under light microscope. Xerogels were prepared by drying the samples under vacuum followed by sprinkling of a mixture of acetone and hexane (7 : 3) on the dried sample. This treatment helped in the complete removal of the apolar phase from the gelled structure without disturbing the networked structure formed by the gelator molecules. This procedure helped in the imaging of the xerogels, which in turn, provided information about the morphology of the networked structure.¹⁸ SEM analysis of GW showed a dense network of fibers forming a three dimensional mesh-like structure [Figure 6(a)], which entrapped the apolar liquid within the interspaces by surface tension and capillary forces.¹⁹ On the other hand, the micrograph of GW xerogel [Figure 6(b,c)] showed uniformly distributed vesicular spherical and tubular structures, which contained water.²⁰ The surface of these vesicular structures showed fibers of SM indicating that the water droplets have been protected from the external apolar phase by a layer of SM.

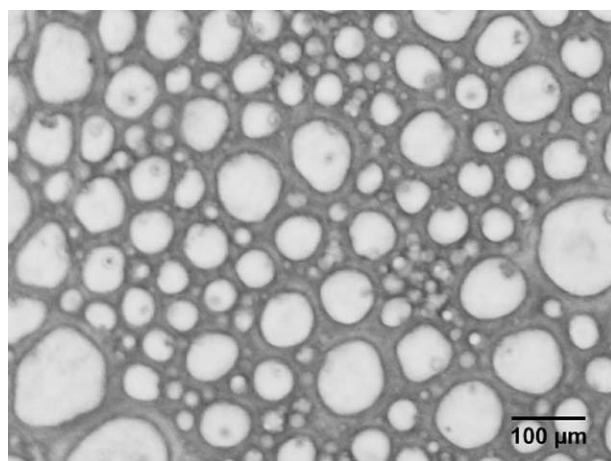


Figure 5. Micrograph of GW gel.

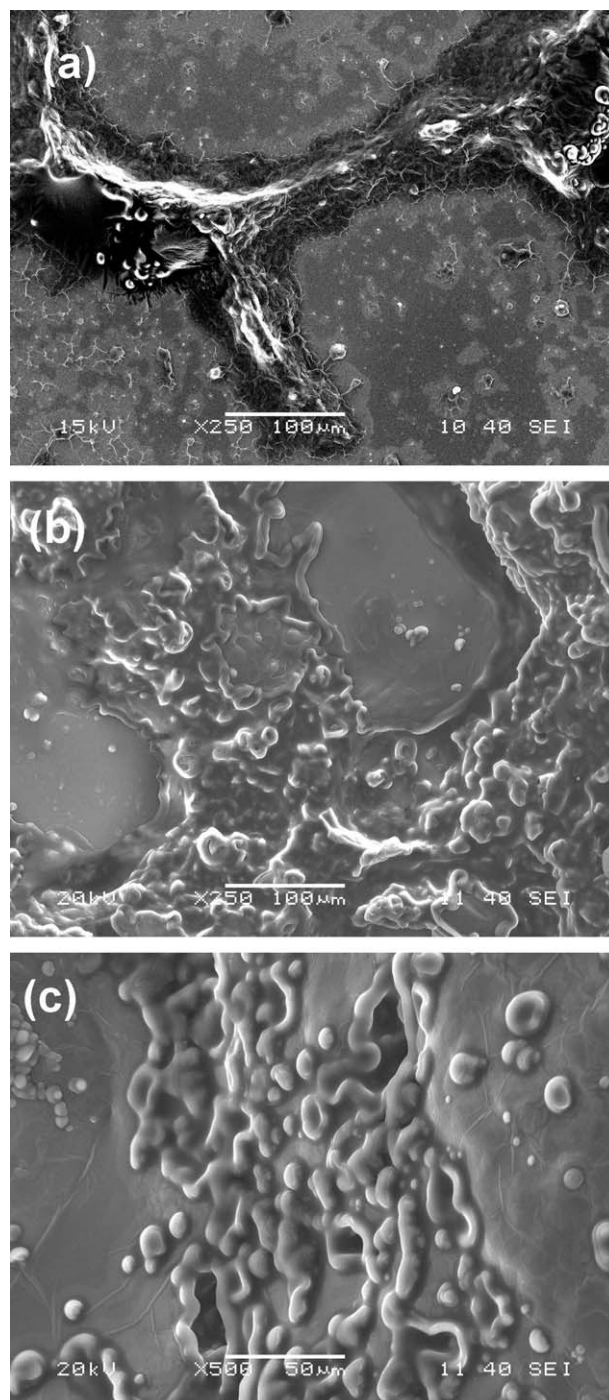


Figure 6. Scanning electron micrographs of the organogels. (a) G showing a branch of fibers, (b) GW showing spherical and tubular vesicular structure, and (c) GW under higher magnification.

FTIR Spectroscopy

Fourier transform infrared (FTIR) studies gives information about the nature of interactions (Figure 7). SO showed an absorption peak at 3008 cm^{-1} , which may be associated with the stretching vibration of *cis* olefinic, CH double bond present in fatty acids.²¹ The absorption peaks at 2920 cm^{-1} and 2850 cm^{-1} was due to CH asymmetric stretch in CH_3 and CH_2 and

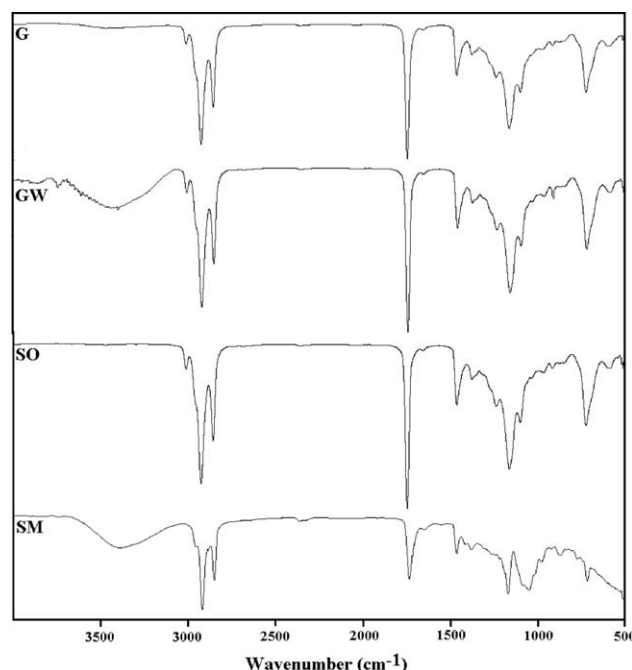


Figure 7. FTIR of (a) SM, (b) SO, (c) GW, and (d) G.

CH symmetric stretch in CH_2 and CH_3 , respectively. This indicated the presence of highly ordered trans zig zag conformation of aliphatic hydrocarbon chain in the SO.²² Absorption near 1743 cm^{-1} indicated the presence of stretching vibration of CO, in the ester group of triglycerides present in sunflower oil.²³ The CH_2 and CH_3 scissoring vibrations were observed at 1460 cm^{-1} and 1373 cm^{-1} .²⁴ A peak at 720 cm^{-1} was due to rocking and wagging of CH_2 in SO. Absorption near 1733 cm^{-1} in SM indicated the carbonyl absorption of ester group. SM showed an absorption peak at 1172 cm^{-1} , which may be attributed to the CO symmetric stretching vibration due to the sugar group present in SM. Intramolecular hydrogen bonding amongst the SM molecules was confirmed by the presence of an absorption peak at 3391 cm^{-1} . The gels showed a less intense peak at 3391 cm^{-1} indicating the presence of the intermolecular hydrogen bonding amongst the gel components. A shift to higher wavenumber (2922 cm^{-1} and 2853 cm^{-1}) of CH asymmetric stretch in CH_3 and CH_2 and CH symmetric stretch in CH_2 and CH_3 , respec-

Table I. Gel–Sol Transition Temperature of G and GW

Temperature	G	GW
35°C	Gel phase	Gel phase
40°C	Gel phase	Gel phase
45°C	Structural integrity compromised	Gel phase
50°C	Opaque liquid	Gel phase
55°C	Clear liquid	Gel phase
60°C	Clear liquid	Gel phase
65°C	Clear liquid	Gel phase
70°C	Clear liquid	Gel phase
75°C	Clear liquid	System starts flowing

tively in gels showed the presence of gauche conformers in the hydrocarbon chain, which is often associated with the high degree of disorderness.¹⁹

Gel–Sol Transition Temperature

T_{gs} was determined by inverted tube method. The temperatures of the samples were increased from 35°C to 80°C at an increment of 5°C and the results have been tabulated in Table I. As the temperature was increased, there was a change in solubility parameter of the SM thereby resulting in the increase in the solubility of the SM molecules. This, in turn, resulted in the increased kinetic energy of the gelator molecules and subsequent decrease in the intermolecular hydrogen bonding, responsible for the self-assembly of the gelator molecules. Hence, due to the increase in the solubility of the gelator molecules as the temperature was increased, there was a subsequent disruption of the networked structure and the gels started flowing. The results indicated that G gel had a lower T_{gs} as compared to GW gel. The increased T_{gs} of the GW gel have been attributed to the formation of stable networked structures due to the increased hydrophobic interactions, which promoted the self-assembly of the gelator molecules. The increase in the hydrophobic interactions is due to the expansion of the micellar structures with the addition of aqueous phase.²⁵

XRD Analysis

The diffractograms of the samples were analyzed using Xpert high score (version 1.0b, Philips analytical B.V.). The X-ray diffraction (XRD) pattern of SM and gels have been shown (Figure 8). XRD of SM showed a sharp peak at $21^\circ 2\theta$, corresponding to a Bragg distance (d -spacing) of 4.154 \AA , indicating the crystalline nature of the gelator. G gel showed a hump at $\sim 20^\circ 2\theta$, indicating that hydrocarbon chains assumed a liquid-like conformation.²⁶ The second peak at $\sim 21^\circ 2\theta$ may be attributed to the presence of SM

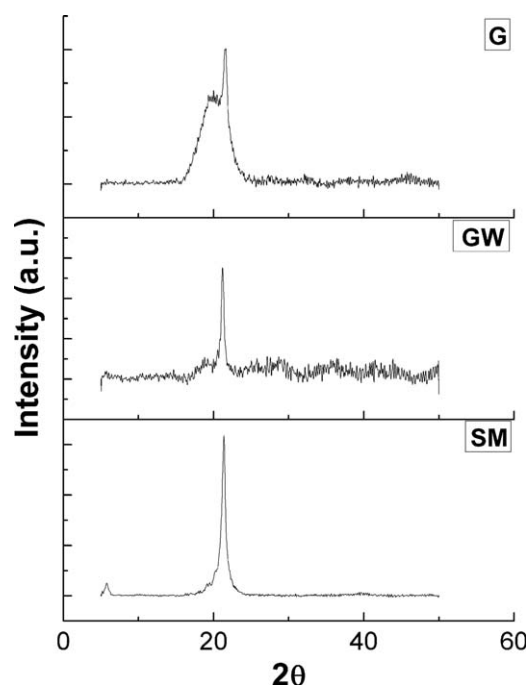


Figure 8. XRD graphs of SM, G, and GW.

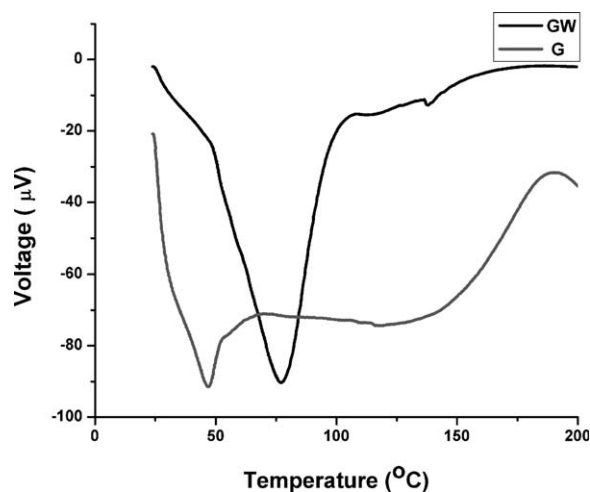


Figure 9. DTA curves of G and GW.

molecules in the gels. Similar to G gel, GW gel also showed a hump $\sim 19^\circ 2\theta$ but the intensity of the hump was quite low. This indicated that the hydrocarbon chains are more rigidly packed in the GW gel. The peak at $\sim 21^\circ 2\theta$ indicated the presence of the SM molecules in the GW gel. From the XRD profiles of the gels, it can be concluded that there is an increase in the crystallinity of the gels as water was incorporated within the gelled structures.²⁷ Hence a higher T_{gs} , as determined by the inverted tube method, was observed in the GW gels. This may be due to the increase in the orderness in the structure of GW gel, responsible for the stability of GW gel as compared to G gel.

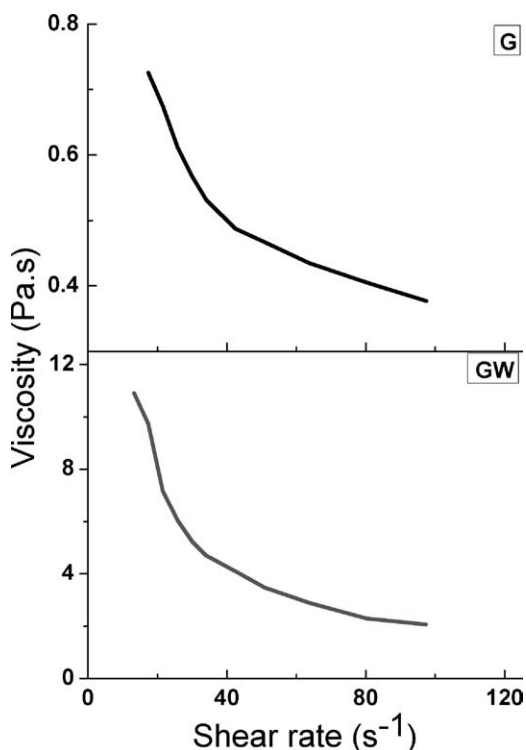


Figure 10. A plot of viscosity vs. shear rate of the gels showing shear thinning behavior.

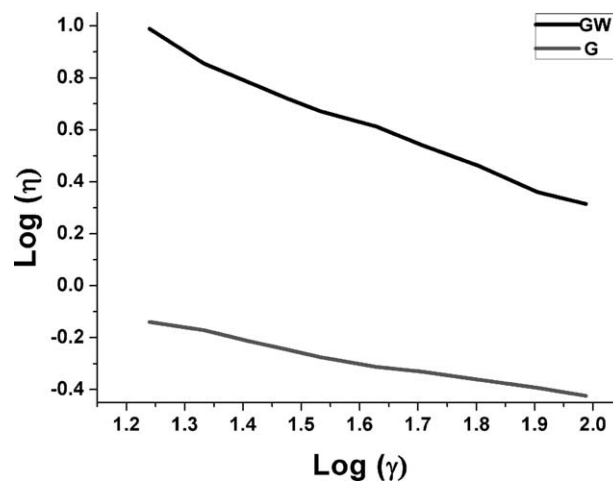


Figure 11. A plot of viscosity vs. shear rate (log-log scale) of the gels.

Thermal Analysis

The thermal behavior of the gels as determined by DTA analysis has been shown in Figure 9. The result showed that the GW gel had a higher melting point when compared to G gel. This is in accordance to the results obtained by T_{gs} determination using inverted tube method and XRD results indicating an increase in the crystallinity of the GW gel. Because of the divergent nature of these gels this method provides a precise result. Thermal analysis showed endothermic peaks at 47°C and 77°C for G and GW gels, respectively.

Rheological Studies

Ostwald–de wale power law mathematical model [eq. (2)] was used to analyze the rheological behavior of the gels.²⁸

$$\eta = K \cdot \dot{\gamma}^{n-1} \quad (3)$$

where, η = shear viscosity, K = consistency index, n = power law index, and $\dot{\gamma}$ = shear rate.

Both the gels showed shear-thinning phenomena, i.e., the viscosity of the gels decreased as the shear-rate was increased (Figure 10). The gels followed a non-Newtonian flow behavior as figured out from the rheological analysis done by the power law equation (Figure 11). For topical gels intended for pharmaceutical and cosmetic applications, shear-thinning phenomenon ensures a formation of thin layer of the formulation over the skin surface which is necessary for efficient delivery of bioactive agents.²⁹ Apart from the above, a higher viscosity at low shear rates ensures long-term stability during storage as the higher viscosity of the formulation reduces the chances of phase separation.³⁰ As evident from the results of FTIR, gel formation also involved hydrogen bonding. Comba and Sethi (2009) reported that these interactions were progressively disrupted

Table II. Power Law Parameters

Gels	Power law index (n)	Correlation coefficient
G	0.63	0.98
GW	0.14	0.999

Table III. Impedance Measurement

Gels	Resistance (M Ω)	Conductance (mho)
G	–	–
GW	0.090563	11.042×10^{-6}
20% gelator + water	0.1275	7.843×10^{-6}
21% gelator + water	0.1353	7.386×10^{-6}
22% gelator + water	0.140	7.142×10^{-6}

under the influence of increased shear stress thereby making the gels to flow.³¹ The viscosity of the GW gel was higher as compared to G gel. This may be attributed to the increase in the hydrophobic interactions amongst the gelator molecules as water was introduced in the GW gel.³² Also, an increase in the rigidity in the gel structure, evident from the XRD results, as water was incorporated within the gelled structure may play an important role in the higher viscosity of the GW gel. The power law indices (n) were calculated from the eq. (2) in the shear rate range of 13.07–97.42 s^{−1} and have been tabulated in Table II. The results showed that $n < 1$, indicating the pseudoplastic rheological behavior of the gels.³³

pH of Gels

There was not much difference in the pH of the samples. The G and GW gels showed a pH range of 6.5 and 6.7, respectively, indicating that the gels might be non-irritant and compatible with skin cells.³⁴

DC Impedance Measurement

The results of gel conductivity have been tabulated in Table III. The G gel did not show any conductivity whereas GW gel showed good electro-conductive property. This was accounted to the formation of conducting aqueous channels in the organogels as was also evident from the light microscopy and scanning electron microscopy.³⁵ To understand the effect of the gelator concentration on the conductivity of the water containing gels, the proportion of gelator was varied in the range of 20% and 22% without altering the water proportion. The results indicated a decrease in the conductivity of the gels as the gelator concentration was increased. This may be attributed to the increase in the resistance to flow of current as the gelator concentration was increased. The preliminary results indicated that the water containing gels may also be tried as matrices for bioactive agents to be delivered by iontophoresis.³⁶

Hemocompatibility Test

Absence of hemolysis is an indication of good hemocompatibility.³⁷ The % haemolysis indicates the extent of lysis of red blood cells when kept in contact with blood. The results of the study have been tabulated in Table IV. Both the samples were found to be acceptable as blood compatible and may be regarded as biocompatible based on the preliminary study.³⁸

Table IV. Hemocompatibility Studies

Sample	% Hemolysis
G	1.8 ± 0.25
GW	1.7 ± 0.67

Table V. Antimicrobial Studies

Samples	Zone of inhibition (cm)
Ciprofloxacin	2.0 ± 0.21
G	0.8 ± 0.15
GW	0.7 ± 0.14
GWD	1.9 ± 0.14

Antimicrobial Studies

On storage of GD gels, the drug incorporated within the gelled structure migrated toward the surface of the gel which is a marker for instability of the formulation. Hence, the GD gels were not used for the antimicrobial studies. The drug alone was used as positive control. The results of antimicrobial activity have been tabulated in Table V. The study showed that the G and GW gels had a mild activity against *B. subtilis*. Also, the drug loaded gels were able to restrict the growth of the microorganisms in the surrounding area of the formulation and did not allow the growth of microorganisms even after 24 h.

Stability Studies

G gels showed syneresis after 4 months upon storage at 25°C/60% RH. GW gels did not show any syneresis even after 1 year suggesting that addition of water improved the stability to a greater extent. This was due to the increased orderliness of GW gels as confirmed by XRD studies which is due to the increase in the intermolecular hydrogen bonding, ascertained by the FTIR results.

CONCLUSIONS

The present study indicated that incorporation of water into the SM organogels produced mechanically stronger gels and exhibited a higher thixotropic behavior. Addition of water also increased the stability of the gels which is due to the increase in the intermolecular hydrogen bonding. This, in turn, improved the molecular packing of the components within the gel structure. The conductivity of these gels may allow them to be used as efficient vehicle for iontophoretic drug-delivery systems.^{36,39} These gels tend to form emulsion which can be used as a vehicle for hydrophilic, lipophilic, and amphiphilic agents.^{17,40} The use of edible oil rich in unsaturated fatty acid in gel formation can serve as a substitute for many food supplements.^{41,42} Recent literatures indicate that probiotics entrapped within the inner aqueous phases of the emulsions improve the stability of the probiotics in the gastrointestinal tract.⁴³ Hence, the water containing gels may improve the survival proportion of probiotics in the gut by protecting them from the harsh acid and bile environment when consumed orally.⁴³ The easy method of preparation of the organogels as compared to the formulation of the other semi-solid formulations (e.g., ointments, creams, and lotions) may allow the scaling up the production easily. Also, the production of organogels is cost-effective. These gels can be used as model span 40 based organogels, for predicting the thermal behavior span 40 based organogels. This helps in understanding the thermodynamic properties and structural arrangement of the gels.⁴⁴ In short, the water-incorporated gels

have got a potential to be used in the pharmaceutical, nutraceutical, and cosmetic industries.

ACKNOWLEDGMENTS

The leading author acknowledges the financial support extended to her by National Institute of Technology, Rourkela for the completion of Ph.D program. The authors thank Prof. K. Pramanik, Department of Biotechnology and Medical Engineering and Prof. S. Paria, Department of Chemical Engineering for providing access to their viscometer facilities. The funds leveraged from the project (BT/PR14282/PID/06/598/2010) sanctioned by Department of Biotechnology, Government of India is hereby acknowledged.

REFERENCES

- Sawalha, H.; Venema, P.; Bot, A.; Flöter, E.; van der Linden, E. *Food Biophys.* **2011**, *6*, 20.
- Yury, E. S. *Prog. Polym. Sci.* **2011**, *36*, 1184.
- Pasquali, R. C.; Sacco, N.; Bregni, C. *J. Dispers. Sci. Technol.* **2010**, *31*, 482.
- Ren, X.; Yu, W.; Zhang, Z.; Xia, N.; Fu, G.; Lu, X.; Wang, W. *Colloids Surf. A* **2011**, *375*, 156.
- Schäink, H.; Van Malssen, K.; Morgado-Alves, S.; Kalnin, D.; Van der Linden, E. *Food Res. Int.* **2007**, *40*, 1185.
- Cottens, S.; Haebler, B.; Sedrani, R.; Vonderscher, J. U.S. Pat. App. 20,070/208,075 (2007). Available at: <http://www.chemblink.com/products/26266-57-9.htm>.
- Zhao, D.; Huo, Q.; Feng, J.; Chmelka, B. F.; Stucky, G. D. *J. Am. Chem. Soc.* **1998**, *120*, 6024.
- Dassanayake, L. S. K.; Kodali, D. R.; Ueno, S. *Curr. Opin. Colloid Interface Sci.* **2011**, *16*, 432.
- Tolasa, S.; Lee, C. M.; Cakli, S. *J. Food. Sci.* **2010**, *75*, C305.
- Hanabusa, K.; Hirata, T.; Inoue, D.; Kimura, M.; Shirai, H. *Colloids Surf. A* **2000**, *169*, 307.
- Shaikh, I.; Jadhav, S.; Jadhav, K.; Kadam, V.; Pisal, S. *Curr. Drug Deliv.* **2009**, *6*, 1.
- Maity, G. C. *J. Phys. Sci.* **2007**, *11*, 156.
- Li, X. Y.; Kong, X. Y.; Wang, X. H.; Shi, S.; Guo, G.; Luo, F.; Zhao, X.; Wei, Y. Q.; Qian, Z. Y. *Eur. J. Pharm. Biopharm.* **2010**, *75*, 388.
- Bursali, E. A.; Coskun, S.; Kizil, M.; Yurdakoc, M. *Carbohydr. Polym.* **2011**, *83*, 1377–1383.
- Vecino, M.; González, I.; Muñoz, M. E.; Santamaría, A.; Pomposo, J. A. *Polymer* **2003**, *44*, 5057.
- Li, W.-S.; Jia, X.-R.; Wang, B.-B.; Ji, Y.; Wei, Y. *Tetrahedron* **2007**, *63*, 8794.
- Sahoo, S.; Kumar, N.; Bhattacharya, C.; Sagiri, S.; Jain, K.; Pal, K.; Ray, S.; Nayak, B. *Polymers* **2010**, *14*, 95.
- Markovic, N.; Dutta, N. K. *Thermochim. Acta.* **2005**, *427*, 207.
- Luo, X.; Xiao, W.; Li, Z.; Wang, Q.; Zhong, J. *J. Colloid Interface. Sci.* **2009**, *329*, 372.
- You, L.-Y.; Wang, G.-T.; Jiang, X.-K.; Li, Z.-T. *Tetrahedron* **2009**, *65*, 9494.
- Muik, B.; Lendl, B.; Molina-Diaz, A.; Valcarcel, M.; Ayora-Cañada, M. J. *Analyt. Chim. Acta.* **2007**, *593*, 54.
- Ifuku, S.; Tsujii, Y.; Kamitakahara, H.; Takano, T.; Nakatsubo, F. *J. Polym. Sci. Part A: Polym. Chem.* **2005**, *43*, 5023.
- Pérez-Mateos, M.; Montero, P.; Gómez-Guillén, M. C. *Food Hydrocolloids* **2009**, *23*, 53.
- Atek, D.; Belhaneche-Bensemra, N. *Eur. Polym. J.* **2005**, *41*, 707.
- Bonacucina, G.; Cespi, M.; Mencarelli, G.; Giorgioni, G.; Palmieri, G. F. *Polym.* **2011**, *3*, 779.
- Wang, X.; Zhou, L.; Wang, H.; Luo, Q.; Xu, J.; Liu, J. *J. Colloid Interface Sci.* **2011**, *353*, 412.
- Bot, A.; Veldhuizen, Y. S. J.; den Adel, R.; Roijers, E. C. *Food Hydrocolloids* **2009**, *23*, 1184.
- Neves, J.; Da Silva, M. V.; Gonçalves, M. P.; Amaral, M. H.; Bahia, M. F. *Curr. Drug Deliv.* **2009**, *6*, 83.
- Evan, M. J. *Non-Newt. Fluid Mech.* **2007**, *141*, 138.
- Yang, Y.; Wang, S.; Xu, H.; Sun, C.; Li, X.; Zheng, J. *Asian J. Pharm. Sci.* **2008**, *3*, 175.
- Comba, S.; Sethi, R. *Water Res.* **2009**, *43*, 3717–3726.
- Maitra, U.; Chakrabarty, A. *Beilstein J. Org. Chem.* **2011**, *7*, 304.
- Fang, P.; Manglik, R. M.; Jog, M. A. *J. Non-Newt. Fluid Mech.* **1999**, *84*, 1.
- Kamble S.R., Udapurkar, P.; Nakhat P. D.; Yeole P., Biyani, K. R. *Indian J. Pharm. Educ. Res.* **2010**, *45*, 65.
- Murdan, S.; Bergh, B.; Gregoriadis, G.; Florence, A. T. *J. Pharm. Sci.* **1999**, *88*, 615.
- Kantaria, S.; Rees, G. D.; Lawrence, M. J. *J. Controlled Release* **1999**, *60*, 355.
- Yang, Z.; Wang, J.; Luo, R.; Maitz, M. F.; Jing, F.; Sun, H.; Huang, N. *Biomaterials* **2010**, *31*, 2072.
- Amarnath, L. P.; Srinivas, A.; Ramamurthi, A. *Biomaterials* **2006**, *27*, 1416.
- Semalty, A.; Semalty, M.; Singh, R.; Saraf, S. K.; Saraf, S. *Technol. Health Care* **2007**, *15*, 237.
- Willmann, H.; Walde, P.; Luisi, P.; Gazzaniga, A.; Stropolo, F. *J. Pharm. Sci.* **1992**, *81*, 871.
- Mulokozi, G.; Bilotta, S. *Immunology* **1999**, *97*, 595.
- Sanders, T. A. B. *Am. J. Clin. Nutr.* **2000**, *71*, 176S.
- Shima, M.; Morita, Y.; Yamashita, M.; Adachi, S. *Food Hydrocolloids* **2006**, *20*, 1164.
- Erukhimovich, I.; Thamm, M. V.; Ermoshkin, A. V. *Macromolecules* **2001**, *34*, 5653.